



## OPEN ACCESS

## EDITED BY

Hongliu Henry Zeng,  
The University of Texas at Austin, United States

## REVIEWED BY

Luigi Jovane,  
University of São Paulo, Brazil  
Yintao Lu,  
PetroChina Hangzhou Research Institute of  
Geology, China  
Isnianto Saputra,  
Job Pertamina Medco Simenggaris, Indonesia

## \*CORRESPONDENCE

Harya Dwi Nugraha,  
✉ harya.nugraha@uib.no

RECEIVED 18 April 2025

ACCEPTED 27 May 2025

PUBLISHED 12 June 2025

## CITATION

Nugraha HD and Maulin HB (2025) Hybrid  
turbidite–contourite systems in the modern  
Tarakan Basin: seismic sedimentology and  
analogue for subsurface storage.  
*Front. Earth Sci.* 13:1614416.  
doi: 10.3389/feart.2025.1614416

## COPYRIGHT

© 2025 Nugraha and Maulin. This is an  
open-access article distributed under the  
terms of the [Creative Commons Attribution  
License \(CC BY\)](https://creativecommons.org/licenses/by/4.0/). The use, distribution or  
reproduction in other forums is permitted,  
provided the original author(s) and the  
copyright owner(s) are credited and that the  
original publication in this journal is cited, in  
accordance with accepted academic practice.  
No use, distribution or reproduction is  
permitted which does not comply with  
these terms.

# Hybrid turbidite–contourite systems in the modern Tarakan Basin: seismic sedimentology and analogue for subsurface storage

Harya Dwi Nugraha<sup>1,2\*</sup> and Hade Bakda Maulin<sup>3</sup>

<sup>1</sup>Department of Earth Science, University of Bergen, Bergen, Norway, <sup>2</sup>Center for Sustainable Geoscience and Outreach (CSGO), Universitas Pertamina, Jakarta, Indonesia, <sup>3</sup>Regional New Ventures, Pertamina Hulu Energi (PHE), Jakarta, Indonesia

Hybrid turbidite–contourite systems are present where gravity-driven and bottom-current processes interact. Although recent studies have advanced our understanding, deciphering the relative roles of downslope and alongslope processes in shaping the deep seafloor remains an important subject of investigation. The Tarakan Basin, offshore northeastern Borneo, is a prolific hydrocarbon province, yet its modern sedimentary systems are poorly understood. Shaped by rapid deltaic sedimentation, active tectonics, and ocean currents—the South China Sea Throughflow (SCSTF) and Indonesian Throughflow (ITF) – the basin offers an ideal setting to study hybrid deepwater processes. Here, we conducted seismic sedimentology analysis to quantify morphometric parameters, delineate seismic facies, and interpret depositional processes using 3D seismic reflection data. Three segments are identified. The Northern Segment is dominated by upslope-migrating sediment waves and plastered drifts, indicative of contourite-dominated conditions. The Central Segment hosts a canyon–drift complex, formed by synchronous interaction of turbidity flows and bottom currents. In contrast, the Southern Segment is shaped mainly by turbidity currents, with gullies and associated sediment waves suggesting limited bottom current influence. These spatial variations reflect a spectrum of hybrid depositional styles, consistent with global models of contourite-, synchronous-, and turbidite-dominated systems. The sedimentary patterns observed provide an analogue for subsurface reservoir and seal distribution, relevant to both petroleum and carbon storage systems.

## KEYWORDS

Tarakan Basin, hybrid systems, bottom currents, turbidity currents, seismic sedimentology

## 1 Introduction

Seabed geomorphology reflects the dynamic interplay of sedimentary processes on the ocean floor. Decades after foundational studies in deep-marine environments (e.g., [Ericson et al., 1952](#); [Hollister and Heezen, 1972](#)), a detailed understanding of seafloor processes remains critical for a range of applications, from geohazard risk assessment and infrastructure site selection

to the exploration of subsurface storage systems, such as for carbon capture and storage (CCS) (e.g., Amjadian et al., 2023; Warchol et al., 2025). In highly dynamic sedimentary environments, where episodic flows and persistent bottom currents interact along continental slopes, interpreting geomorphological patterns is crucial for reconstructing sedimentary system evolution (e.g., Bailey et al., 2024; Nugraha et al., 2019).

On continental margins, seafloor morphology is shaped by the interplay of gravity-driven (downslope) and current-driven (alongslope) sedimentary processes (Kiswaka et al., 2025; Rebesco et al., 2014; Rodrigues et al., 2022b). These processes often interact, creating hybrid depositional systems marked by complex and laterally variable geomorphology (Fuhrmann et al., 2022; Miramontes et al., 2020; Rodrigues et al., 2022b). Examples of such interactions are observed in both ancient and modern continental margins worldwide, including the offshore Argentina (Rodrigues et al., 2022a), offshore Brazil (Alves et al., 2023; Schattner et al., 2024), offshore NW Africa (Mourlot et al., 2018), offshore East Africa (Fuhrmann et al., 2022; Kiswaka et al., 2025; Lu et al., 2021a), South China Sea (Gong et al., 2015; Liu et al., 2022; Palamenghi et al., 2015; Alves et al., 2023), offshore NW Australia (Nugraha et al., 2019), offshore SE Australia (Harishidayat et al., 2024; Wu et al., 2024), and the Makassar Strait (Brackenridge et al., 2020). The analysis of hybrid turbidite–contourite systems has become essential in seismic sedimentology and sequence stratigraphy, providing analogues for paleoenvironmental reconstruction and improving predictions of subsurface reservoir and seal distributions (Fonnesu et al., 2020; Fuhrmann et al., 2022; Gong et al., 2016; Rodrigues et al., 2022b; Sansom, 2018). Recognizing the relative contributions of each process is particularly important in deep-water environment exploration, where reworked turbidites and contourite drifts can both act as potential reservoir facies (Fonnesu et al., 2020; Kiswaka et al., 2025; Liu et al., 2022; Sansom, 2018).

The Tarakan Basin, offshore northeastern Borneo, has long been recognized as a product of rapid sedimentation delivering thick deltaic and deep-marine deposits to the slope and basin floor (Figure 1A; Erdi et al., 2023; Krisnabudhi et al., 2022; Lunt and Madon, 2017; Maulin et al., 2019; Morley et al., 2017). During the Plio-Pleistocene, sedimentation rates exceeded 820 m/my on the shelf and approximately 300 m/my on the basin floor (Hidayati et al., 2007; Lentini and Darman, 1996). This contrast in sedimentation is influenced by gravity-driven tectonics, that was initiated since Middle Miocene, where growth faults in the upslope areas trap sediments, while toe-thrust structures in the downslope regions create accommodation for sediment gravity flows deposits (Figure 1B; Erdi et al., 2023; Krisnabudhi et al., 2022; Maulin et al., 2019; Morley et al., 2017; Sapiie et al., 2021). In addition to the downslope processes, the basin is also influenced by an interaction between margin-parallel bottom currents, i.e., the South China Sea Throughflow (SCSTF) and the Indonesian Throughflow (ITF) (Fan et al., 2013; Wei et al., 2016; Xu and Malanotte-Rizzoli, 2013), which have the potential to rework and redistribute sediment along the slope. Despite this, the interactions between downslope and alongslope processes in the Tarakan Basin remain poorly understood, and their seismic expression on the modern seafloor has yet to be comprehensively assessed.

In this study, we aim to characterize the lateral variability of modern seabed features in the slope area of the Tarakan Basin. Our objective is to provide an initial insight on the relative roles of downslope and alongslope processes in shaping the basin's seafloor and identify key seismic sedimentology indicators of hybrid turbidite–contourite systems. The results provide insights not only into present-day sedimentary dynamics, but also into the stratigraphic architecture of analogous systems in deeper intervals, with implications for the prospectivity of both petroleum and carbon storage systems.

## 2 Geological setting

The Tarakan Basin is located on the northeastern margin of Borneo, Indonesia, within a structurally complex region shaped by the interaction of regional subduction and strike-slip faulting (Hall and Nichols, 2002). It is bounded by the Sampoerna Fault Zone (SFZ) to the north and the Mangkalihat Fault Zone (MFZ) to the south (Figure 1A), with internal segmentation that include NW-trending, Sebatik (SA), Ahus (AA), Bunyu (BA), and Tarakan (TA) arches (Figure 1A; Erdi et al., 2023; Hidayati et al., 2007; Krisnabudhi et al., 2022; Lentini and Darman, 1996; Maulin et al., 2019). These structures resulted from the basin's tectonic evolution that has been governed by Paleogene to Neogene lithospheric deformation, including the counter-clockwise rotation of Borneo (Advokaat et al., 2018), rifting in the Makassar Strait (Satyana, 2015), and uplift associated with the Sabah orogeny (Lunt and Madon, 2017).

Since the Early Miocene (~17 Ma), sedimentation rates increased progressively, from c. 60 to 330 m/my in the Late Miocene (Hidayati et al., 2007). This rapid accumulation of sediments both initiated and was later modulated by delta-related gravitational tectonic deformation (Erdi et al., 2023; Hidayati et al., 2007; Krisnabudhi et al., 2022; Maulin et al., 2019; Sapiie et al., 2021). Facilitated by underlying Miocene mobile shale, the system is composed of growth normal faults trapping fluvial to shallow marine deposits updip, and toe-thrusts ponding gravity-driven deposits downdip (Figure 1B). During the Plio-Pleistocene, sedimentation rates exceeded 820 m/my on the shelf and approximately 300 m/my on the basin floor (Hidayati et al., 2007; Lentini and Darman, 1996). The system is fed by five rivers (Figure 1A), that were redirected by progressively uplifted areas (e.g., BA and TA, see Figure 1A), resulting in bifurcation before reaching the open sea. This bifurcation led to lateral variations of sedimentation rates, which in turn influenced slope processes, contrasting with the focused sedimentation observed in systems like the Mahakam River (Maulin et al., 2019).

Oceanographic setting of the Tarakan Basin is as complex as its geological setting. The basin serves as the confluence area of the South China Sea Throughflow (SCSTF) and the Indonesian Throughflow (ITF, see inset in Figure 1A), whose interaction modulates bottom-current dynamics and sediment dispersal along the slope (Fan et al., 2013; Fang et al., 2009; Wei et al., 2016). The SCSTF developed more recently, becoming active in the early Holocene (~10 ka) following sea-level rise that re-flooded the Sunda Shelf (Fan et al., 2018), whereas the ITF was initiated in the Early Miocene (~23 Ma) and reached its modern configuration in



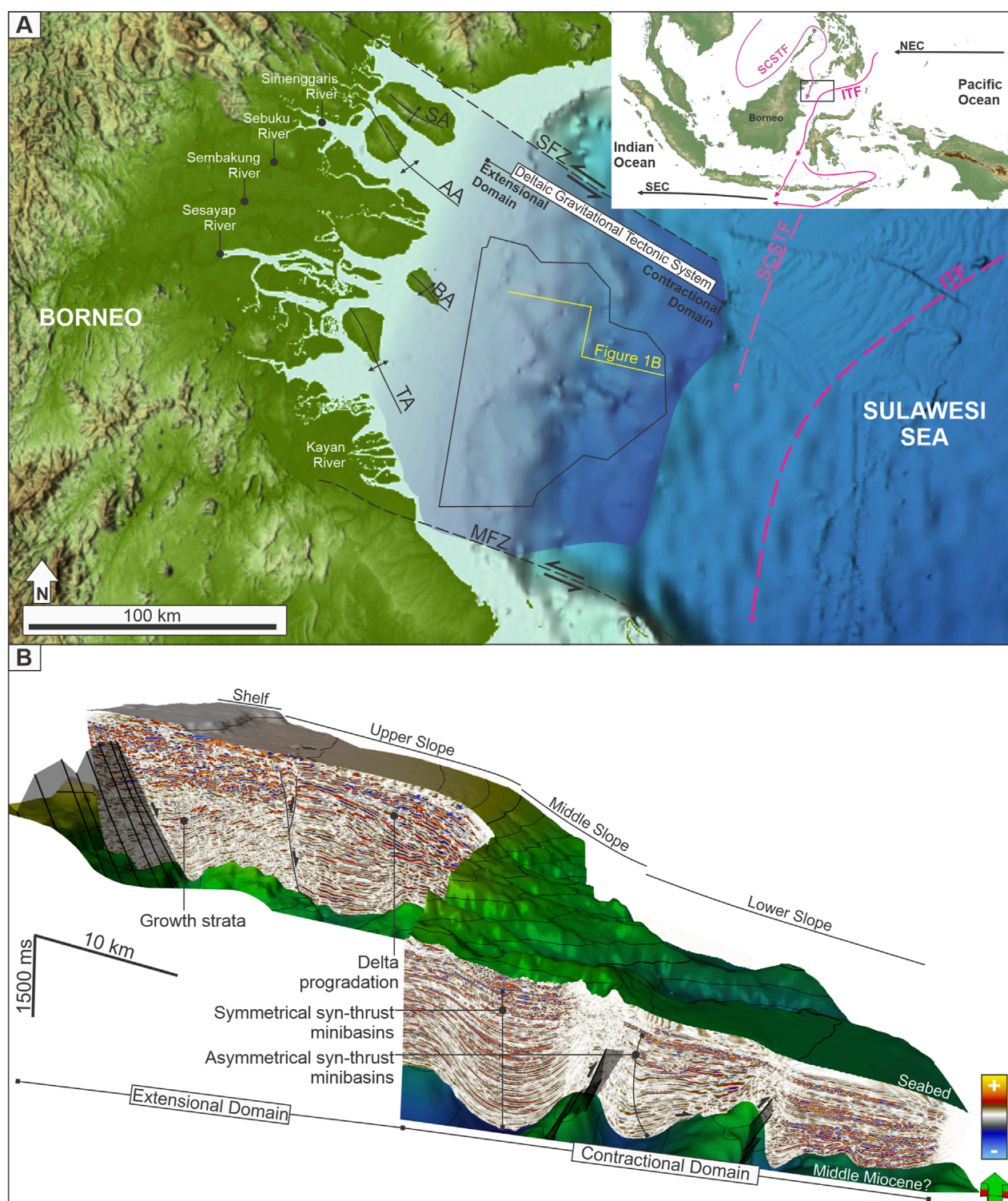


FIGURE 1

(A) Regional map showing the location of the Tarakan Basin and its major structural features (compiled from Erdi et al., 2023; Hidayati et al., 2007, and references discussed in the text). Inset highlights ocean current circulation in the region, including the South China Sea Throughflow (SCSTF), Indonesian Throughflow (ITF), North Equatorial Current (NEC), and South Equatorial Current (SEC) (adapted from Wei et al., 2016). (B) 3D perspective view of the seismic volume displaying the Middle Miocene surface and the modern seabed. The image illustrates the delta-fed gravitational tectonic system of the Tarakan Basin, including the extensional domain with growth faults associated with rapid sedimentation, and the compressional domain characterized by the toe-thrusts. SFZ, Sampoerna Fault Zone; MFZ, Maratua Fault Zone; SA, Sebatik Arch; AA, Ahus Arch; BA, Bunyu Arch; TA, Tarakan Arch. Bathymetry data is from GEBCO 2024 (available at <https://download.gebco.net/>).

the late Pliocene (~2.7 Ma) (Gallagher et al., 2024). SCSTF flows seasonally from the South China Sea through shallow straits into the Sulawesi Sea, primarily within the surface and upper thermocline (0–400 m) (Trinh et al., 2024), while the ITF flows persistently southward from the Pacific through the Sulawesi Sea and Makassar Strait, with most transport concentrated in the thermocline above ~680 m (Gordon, 2005; Susanto and Gordon, 2005). At intermediate depths (~700–1,350 m), the Pacific water enters the Sulawesi Sea by overflowing a bathymetric barrier in the east (i.e., Sangihe Ridge), forming a distinct water mass shaped by bathymetric constraints, internal tides, and vertical mixing (Gordon et al., 2003; Hermansyah et al., 2019; O'Driscoll and Kamenkovich, 2009). Below the barrier depth (>1,350 m), deep water is isolated by surrounding bathymetric barriers encircling the Sulawesi Sea, with weaker along-slope currents and low oxygen indicating long residence time (Gordon et al., 2003; O'Driscoll and Kamenkovich, 2009). ITF can transport sediments and modify seabed morphology, playing a key role in sediment reworking and the formation of contourite features. For instance, adjacent to the Mahakam Delta, Brackenridge et al. (2020) demonstrated that the ITF also acted as a preconditioning factor for submarine landslides in the Makassar Strait.

In this study, we examine the seabed geomorphology and near-surface sedimentary architecture along the slope of the Tarakan Basin, offshore northeastern Borneo. The basin receives sediment from river-fed deltas and is influenced by alongslope oceanographic currents, offering a dynamic setting for investigating the interaction between downslope and alongslope processes. The combination of active tectonics, high sediment supply, and oceanographic forcing makes the Tarakan Basin as a natural laboratory for studying hybrid turbidite–contourite systems.

### 3 Data and methods

This study utilizes 3D reflection seismic data encompass an area of approximately 6,000 km<sup>2</sup> (Figure 2). These data are Post-stack Time Migrated (PSTM) with normal polarity (where an increase in acoustic impedance downwards is indicated by a positive amplitude). The seismic bin spacing is 25 m × 12.5 m (inline × xline), with a 4 ms sampling rate. With dominant frequency of 30 Hz and a velocity of 1,700 m/s in the shallow interval (Erdi et al., 2023), the vertical resolution at the interval of interest is c. 14 m. There are lineations that represent acquisition or processing artifacts that could be clearly identified (Figure 2A). A data gap is present in the central part of the study area, where seismic data is unavailable, thus the mapping within this area is an interpolation of the surrounding bathymetric data (GEBCO Gridded Bathymetry Data 2024; available at <https://download.gebco.net/>).

We interpret the seafloor from the 3D seismic reflection data, which is expressed as the first positive event. The map was then converted to depth using the velocity of seawater, 1,500 m/s. Qualitative analysis was conducted to characterize the morphology of the features (e.g., cross-sectional and plan-view geometries), aided with Dip Magnitude seismic attributes (Figure 2B) that highlight dip variability and lateral continuity (Brown, 2011). In addition to morphology, seismic facies are also characterized in terms of their internal reflection configuration, continuity, amplitude and frequency (Figure 3). Morphometric parameters

were quantitatively measured for key geomorphic features across the study area, including: (i) submarine canyons (width, incision depth, and length); (ii) gullies (length, width, spacing, and incision depth); and (iii) sediment waves (wavelength, amplitude, and orientation). To compare the morphometric distribution of these features, we plot width versus incision depth for submarine canyons and gullies (Figure 4A), and wavelength versus amplitude for sediment waves (Figure 4B). Insights from seismic geomorphology and the corresponding facies are integrated to infer process interactions in the study area.

## 4 Results and interpretation

Seismic data reveal three distinct slope morphologies and associated subsurface architectures between depths of 500 and 2,000 m below sea level (Figures 2, 3). The slope maintains a consistent north–south orientation, but its morphology varies laterally—ranging from the smooth seabed of the Northern Segment, to a radial network of incised submarine canyons in the Central Segment, and transitioning into the steeper terrain in the Southern Segment (Figure 2).

### 4.1 Northern segment

#### 4.1.1 Observation

The Northern Segment displays four primary geomorphic features (Figure 5A): gullies, submarine canyons, sediment waves, and plastered drifts. Gullies are located on the mid to lower slope and vary in geometry and spacing (Figure 5A). In the northern part of this segment, two gullies (6 km long, 0.8–1 km wide) originate from a headscarp and feed into a submarine canyon. In contrast, southern gullies initiate downdip from the western sediment waves field, are ~3 km long, ~300 m wide, and regularly spaced. Additional gullies in between display moderate lengths (3–6 km), widths (300–800 m), and spacing (400–600 m), with no apparent upslope connection to sediment waves. All gullies exhibit V-shaped cross-sections (Figure 3) with incision depths ranging from 30 to 75 m (Figure 4A).

Submarine canyons are present on the lower slope, where only the canyon heads are imaged (Figure 5A). These canyons originate from the downdip end of the plastered drift and are fed by converging gullies. Each canyon head comprises feeder canyons (~800 m wide, 120 m deep) that merge into a larger canyon (3.5 km wide, 150 m deep; see Figure 4A). Seismic facies reveal southward migration of thalwegs (Figure 5B) and increased incision where the feeder canyons merge.

Two clusters of sediment waves are observed on the upper slope (Figures 5A,C). The eastern field consists of 3–4 km-long waves with wavelengths of 300–600 m, curving from a north–south to a northwest–southeast orientation. The western field shows waves of similar length (~5 km) but shorter wavelengths (~200 m). In cross-section, the eastern (large) waves exhibit amplitudes ranging from <15 m in the north to 15–50 m in the south and show asymmetric, upslope-migrating forms, whereas the western (small) sediment waves present lower amplitude (Figure 4B). Seismic facies in both fields are characterized by layered, undulating reflections indicating lateral migration (Figure 5C).



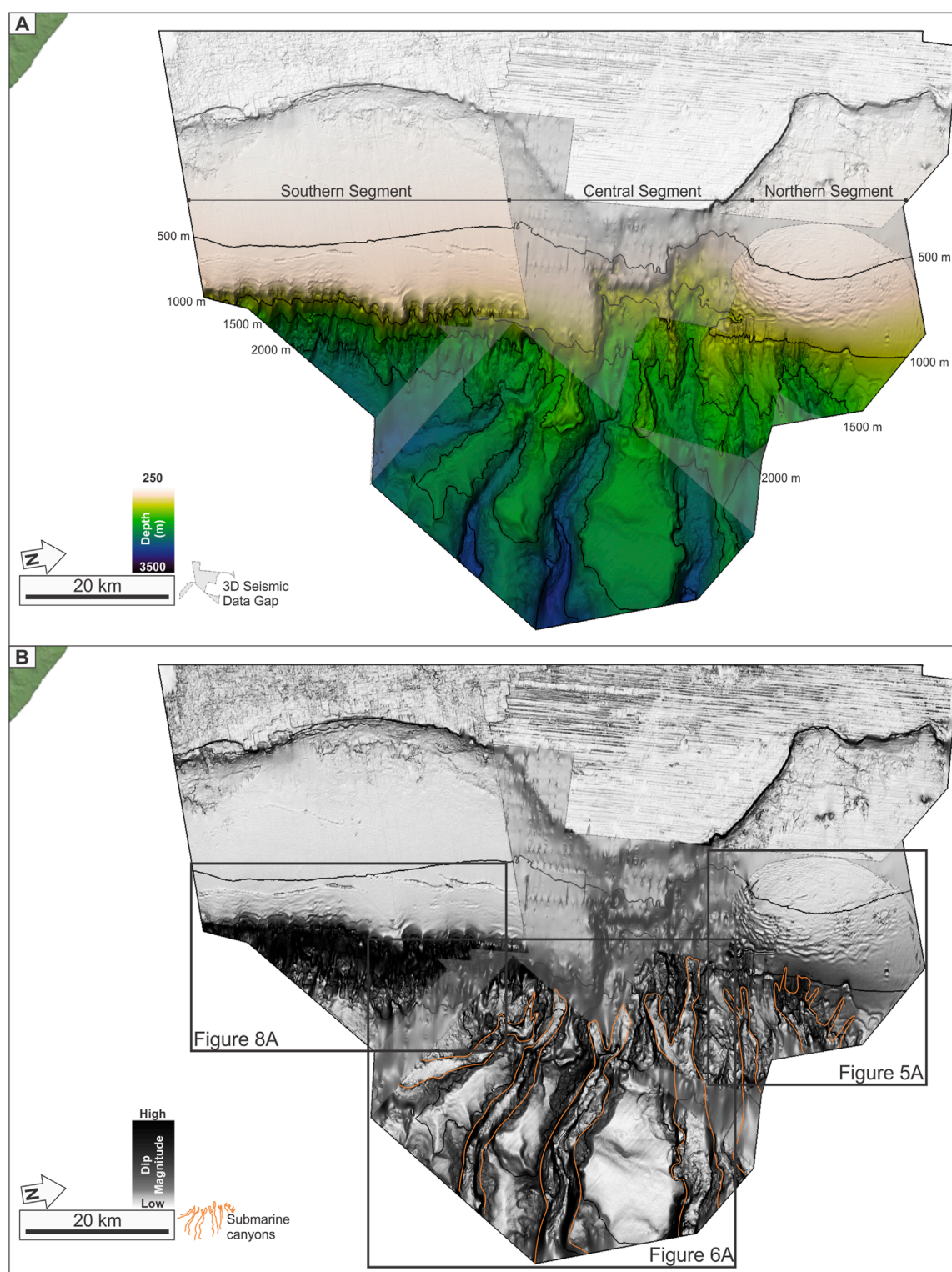


FIGURE 2

(A) Seabed depth map showing the lateral variability of slope morphology across the study area, defining the Northern, Central, and Southern segments. The grey area represents the 3D seismic data gap. (B) Dip magnitude attribute map highlighting slope morphology and sedimentary features. Submarine canyons are outlined in orange.

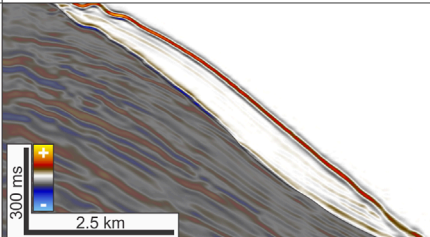
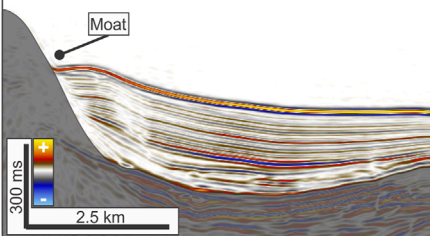
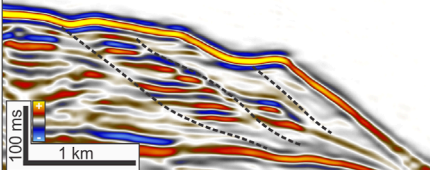
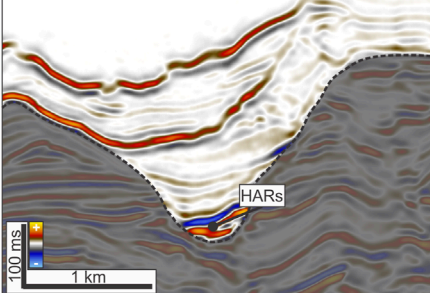
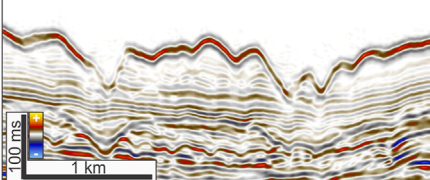
Features	Description	Seismic Facies	Occurrences
<b>Plastered Drift</b>	Sub-parallel, mounded, and semi-continuous internal reflections of low amplitude, bounded by continuous high-amplitude reflections at both the top and base. Typically located along the middle slope.		Northern Segment
<b>Mounded Drift</b>	Sub-parallel, mounded, and continuous internal reflections with alternating low- to high-amplitude character, exhibiting upslope migration. A moat is typically present on the upslope side. Commonly observed on the lower slope.		Central Segment
<b>Sediment Waves</b>	Sub-parallel to wavy, discontinuous to semi-continuous reflections with variable low- to high-amplitude internal reflections. Mainly on the upper slope, but also found on the lower slope.		Northern, Central, and Southern segments
<b>Canyons</b>	Semi-continuous, sub-parallel reflections with alternating amplitudes, often truncated and bounded by U- or V-shaped, high-amplitude basal reflections. Typically initiate on the middle to lower slope, with offset thalwegs indicating lateral migration. High-amplitude reflectors (HARs) occasionally observed filling the canyon axis.		Northern and Central segments
<b>Gullies</b>	Discontinuous to semi-continuous reflections with variable low- to high-amplitude and V-shaped geometry, truncating adjacent reflectors. Typically originate from the upper slope.		Northern and Southern segments

FIGURE 3

Seismic facies characteristics of main sedimentary features found across the three segments.

The plastered drift lies on the middle slope between upslope sediment waves and downslope gullies (Figure 5C). It is elongated (~20 km long), north–south trending, 12 km wide in the north and 6 km wide in the south, with a mounded geometry (~150 m thick) in cross-section. The drift is smooth and lacks an associated moat. Seismic facies show sub-parallel, low-amplitude to transparent reflections, with evidence of incipient slope failures down dip (Figures 3, 5C).

#### 4.1.2 Interpretation

The Northern Segment is interpreted to be primarily shaped by bottom current activity, as evidenced by the extensive plastered drift and associated upslope-migrating sediment waves (Figure 5).

The orientation and geometry of sediment waves, combined with their regular spacing and lateral migration, suggest deposition by sustained, margin-parallel bottom currents. The plastered drift further supports this interpretation, reflecting continuous sedimentation under persistent alongslope flow (Hernández-Molina et al., 2008; Rebesco et al., 2014).

However, the presence of gullies and submarine canyons indicate that gravity-driven downslope processes are also active. The V-shaped geometry and incision of channels, along with their origin near headscarp and convergence into canyons, suggest periodic turbidity flows (Wu et al., 2022). These flows may have been initiated by slope failure and were potentially influenced or confined by existing bottom-current deposits (Brackenridge et al., 2020).



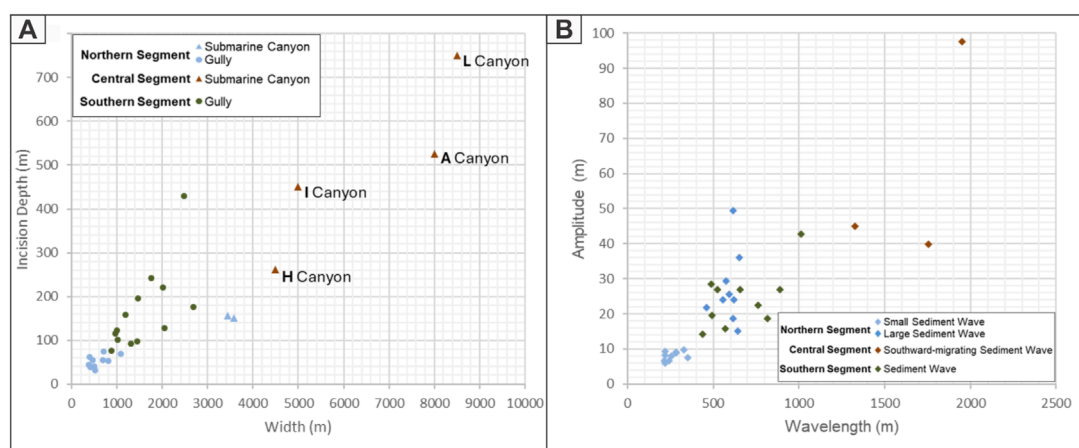


**FIGURE 4**  
Cross-plots showing the morphometric distribution of (A) width versus incision depth for submarine canyons and gullies, and (B) wavelength versus amplitude for sediment waves, shown across the three segments.

Overall, the Northern Segment records a hybrid sedimentary regime, with bottom currents dominating the upper and middle slope, while turbidity currents intermittently shape the deeper slope and canyon systems.

## 4.2 Central segment

### 4.2.1 Observation

In the Central Segment, four submarine canyons originate from a central initiation area located immediately downdip of the shelf (Figure 2). These canyons exhibit radial geometry, forming a fan-like pattern of divergence downslope (Figure 6). In this paper, the four canyons are informally named using words rooted in Bornean languages: from south to north (Figure 6), Harung (“to traverse”), Irang (“dark”), Laju (“continuous flow”), and Arur (“stream” or “watercourse”). These names reflect key processes and settings associated with submarine canyon morphology and the interaction between turbidity and bottom currents. Collectively, they are referred to as the HILA Submarine Canyon Complex.

H Canyon (Harung), the southernmost of the complex, is at least ~25 km long and curves from EW to NNW-trending due to structural buttressing (Figures 6A,B). The cross-sectional geometry of the main canyon varies from symmetric to asymmetric, with width ranges from 3 km updip to 6 km downdip (Figure 6B). The 3 km-wide, 225 m-deep feeder canyon shows westwards offset of thalweg indicating lateral migration that is defined by a thrust fault zone (Figure 7A).

I Canyon (Irang), is NW-trending and at least ~30 km long (Figure 6A). It begins at the lower slope with a ~4 km-wide, 225 m-deep feeder canyon and continues downslope with U-shaped, flat-based cross sections (Figure 6B). The main canyon ranges from 4 to 6 km wide and 300–450 m-deep (Figure 4B). The updip feeder canyon shows southeastward thalweg lateral offsets (Figure 7B).

L Canyon (Laju) is at least ~40 km long and WNW-trending (Figure 6A). The canyon appears to initiate near the shelf, with the presence of feeder canyons inferred from seabed morphology

beyond the updip limit of the 3D seismic coverage. The main canyon ranges from 7 to 10 km in width and 375 to 750 m in depth (Figure 4A). Cross sections reveal a range from symmetrical to asymmetrical V-shaped forms and signs of rotational wall failure (Figure 6B). Cyclic steps appear on the canyon floor (Figure 6C), which are also observed on the floors of the other canyons.

A Canyon (Arur) is at least 42 km-long and extends beyond the seismic survey limits (Figure 6A). The head area features two ~3.5 km-wide feeder canyons that coalesce into an ~8 km-wide canyon downdip, reaching depths of 525 m (Figure 4A). V-shaped geometries in the feeders transition to U-shaped profiles in the main canyon (Figure 6B). The canyon base is mostly flat with terraced walls. Thalweg offsets are noted updip, indicating southwards feeder canyon migration (Figure 7C).

Intercanyon areas between the canyons form triangular zones widening downslope (Figure 6A). The area between H–I canyons hosts EW-trending, southward-migrating sediment waves (5 km-long, 1–2 km spacing, 40–100 m amplitude; Figures 4B, 6A, 7D). I–L and L–A zones contain fault-controlled mounded drifts (Figure 6A). These include moats (~600 m wide, 20 m-deep) and adjacent mounded drifts (8–10 km-long, 6–8 km-wide, 225 m-thick) that thin toward the moats (Figure 7E). Also note that the location of the moats coincides with the underlying thrust fault zones (Figure 7E).

### 4.2.2 Interpretation

The radial configuration of the HILA Submarine Canyon Complex suggests a focused sediment supply over a shelf promontory, where structural highs and toe-thrust anticlines influenced canyon initiation (Figure 6). Structural loading and localized oversteepening likely preconditioned the slope for failure, while tectonic activity acted as a trigger (e.g., Wu et al., 2022).

Canyon orientations relative to the NS-trending thrusts show two modes of structural control: H, I, and L canyons trend across thrusts, likely indicating failure of the anticline crests (e.g., Gee et al., 2007; Nugraha et al., 2020), while A Canyon aligns parallel to thrusts, suggesting lateral confinement during deposition (McGilvery and Cook, 2013).

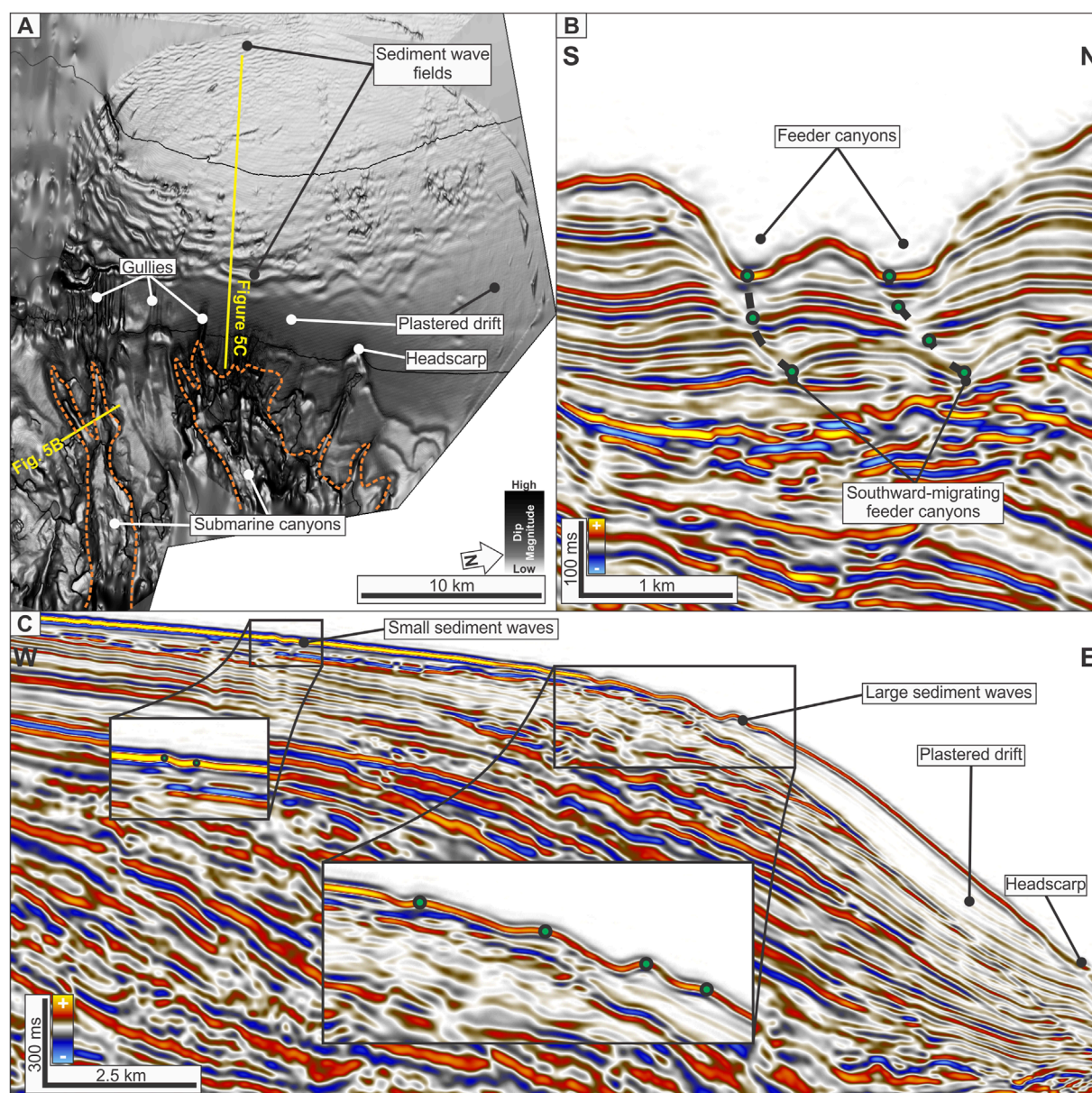


FIGURE 5

(A) Dip magnitude map of the Northern Segment showing sediment waves and plastered drift. The gullies and submarine canyons present downdip from the plastered drift. (B) Seismic section across feeder canyons, illustrating southward-migrating thalwegs (green dots). (C) Seismic section across sediment waves and an associated plastered drift, highlighting upslope-migrating bedforms and mounded drift geometry.

Evidence of bottom-current interaction is observed in updip thalweg offsets (Figures 7A–C), indicating lateral migration of turbidity flows (Alves et al., 2023; Gong et al., 2015). In contrast, cyclic steps downdip highlight the dominance of high-density gravity flows (Figure 6B; Wu et al., 2024). This reflects a transition from hybrid sedimentation in the upper slope to more turbidite-dominated processes downslope.

Intercanyon areas record persistent alongslope transport. Sediment waves in the H–I zone align with canyon bends (Figures 6A, 7D), shows interaction between canyon overspill and bottom current reworking (Lu et al., 2021a; Rodrigues et al., 2022b). Mounded drifts and moats shaped by bottom currents (i.e., likely

by the deep current circulation of the Sulawesi Sea) and structural highs (Figures 6A, 7E). Overall, the Central Segment represents a dynamic interplay between structurally triggered slope failure, turbidity current activity, and modification by bottom current.

## 4.3 Southern segment

### 4.3.1 Observation

The Southern Segment features upslope-migrating sediment waves and a network of gullies (Figure 8A). The sediment waves (wavelength of 430–1,000 m and amplitude of 14–43 m,



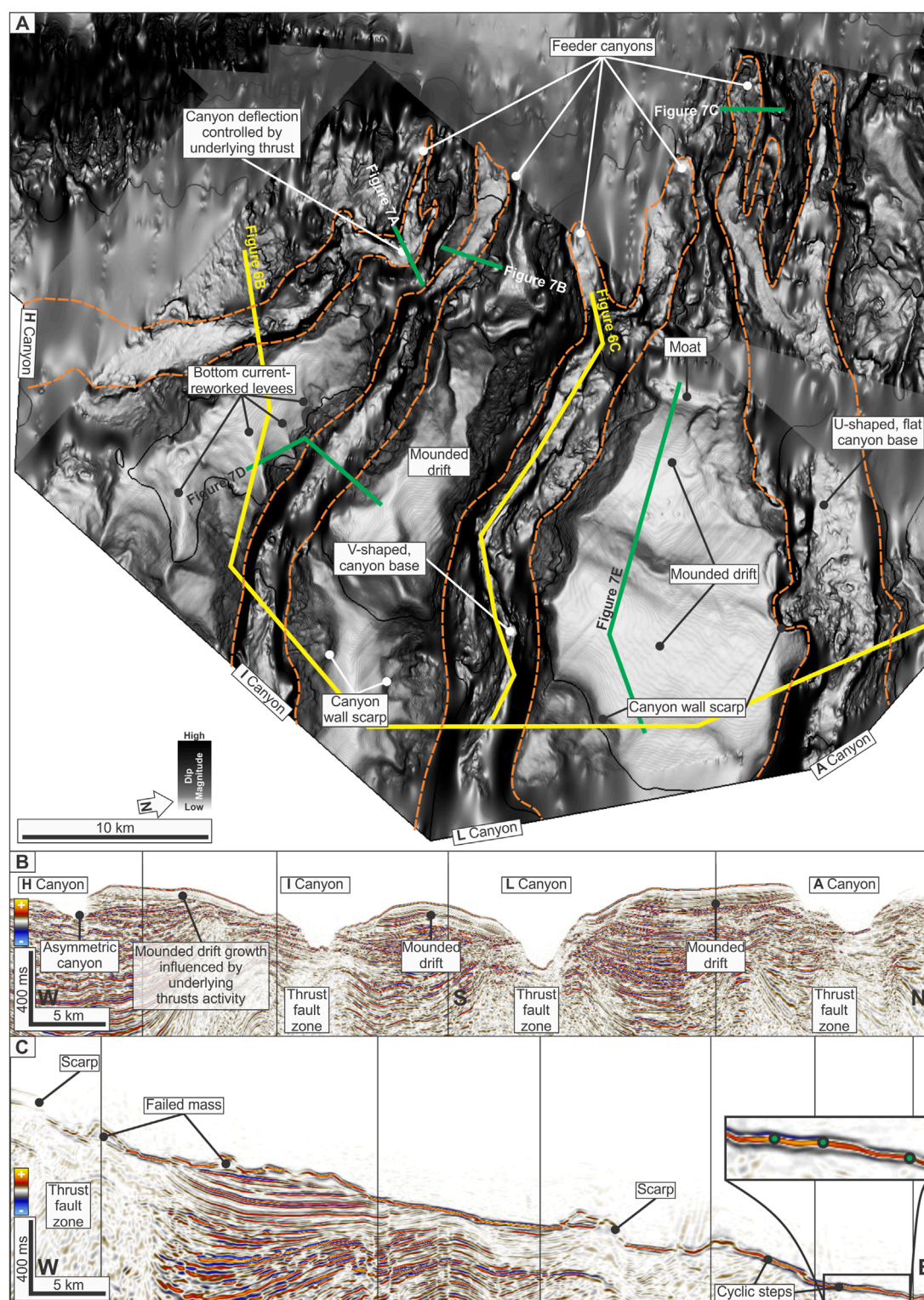


FIGURE 6

(A) Dip magnitude map of the Central Segment, showing the radial arrangement of submarine canyons and associated inter-canyon features (HILA Submarine Canyon Complex). (B) Seismic profile across the canyons, highlighting the cross-sectional geometries and underlying thrust structures. (C) Longitudinal seismic section along the L Canyon, showing scarp of an anticline, failed mass, and internal cyclic steps (green dots represent the crests of cyclic steps).

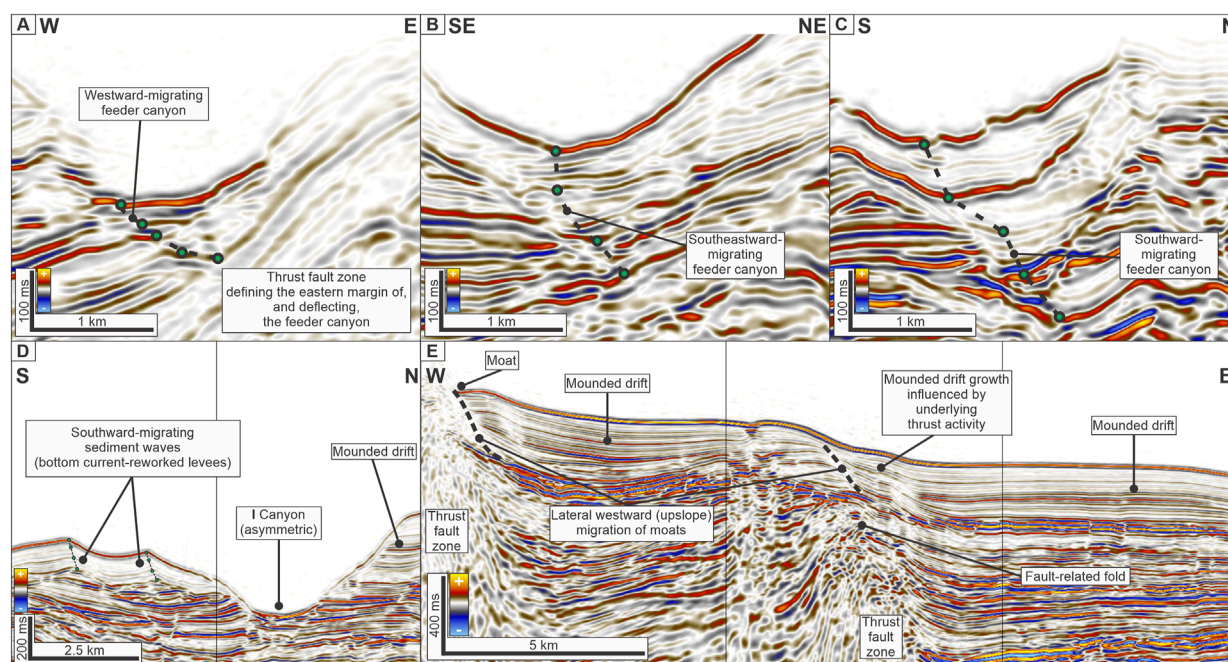


FIGURE 7

Seismic profiles illustrating interactions between downslope and alongslope processes in the Central Segment (see green lines in Figure 6 for section locations). (A) Feeder canyon of H Canyon showing westward migration of the thalweg. (B) Feeder canyon of I Canyon displaying southeastward migration. (C) Feeder canyon of A Canyon with southward-migrating geometry. Green dots in (A–C) represent thalwegs. (D) Asymmetric cross-section of I Canyon, bounded by a mounded drift and southward-migrating sediment waves (green dots represent the crest of sediment waves), interpreted as bottom current–reworked levees. (E) Mounded drifts with associated moats; note the geometrical relationship between the drift body and the underlying thrust fault zone.

see Figure 4B) are observed near the heads of the gullies and predominantly trend north–south as they migrate upslope (Figure 8B). Closer to the gully heads, the waves curve and become subparallel to the gullies (Figure 8A). These wave fields are bounded upslope by three segments of deep normal faults that are still expressed at the seabed (Figure 8A).

Downslope from the sediment waves, a set of gullies extends laterally along the slope for at least 45 km and stretches downslope for up to 10 km, within a depth range of 1,000 and 2,000 m (Figure 8C). The gullies exhibit V-shaped cross-sections with depth ranging from 75 to 450 m and widths of 800–2,500 m (Figure 4A). No notable lateral offset of gully thalwegs is observed (Figure 8D).

### 4.3.2 Interpretation

The proximity between the sediment waves and gullies suggests a potential genetic relationship (Figure 8). The presence of an active delta system (e.g., the Kayan River; see Figure 1) likely supplies mud-rich sediments, which, when combined with fault activity, may have triggered low-density turbidity currents (e.g., Jobe et al., 2011; Lonergan et al., 2013; Lu et al., 2021b). This interpretation is supported by the presence of cyclic steps along the gully thalwegs, indicative of turbidity flows (Wu et al., 2024). While the curvature of the sediment waves near the gully heads may suggest some reworking by bottom currents, the absence of thalweg offset (Figure 8D) supports a model dominated by sheet-like, gravity-driven turbidity currents. Thus, the Southern Segment records the domination of turbidity currents.

## 5 Discussion

### 5.1 Spatial variability of hybrid sedimentary systems in the Tarakan Basin

The Tarakan Basin displays along-strike variability in seafloor geomorphology that reflects the dynamic interplay of downslope gravity flows and alongslope bottom currents (Figure 2). Each segment of the basin exhibits unique combinations of depositional and erosional features, indicating different types of process dominance. Rodrigues et al. (2022b) proposed a classification of hybrid depositional systems into three main categories—contourite-dominated, synchronous, and turbidite-dominated—based on the type of interaction between flows, their lateral migration, and depositional geometries. This framework provides an approach for interpreting the Tarakan Basin's segmental variability.

In the Northern Segment, the predominance of upslope-migrating sediment waves and plastered drifts (Figures 5A,C), and the presence of the southward-migrating feeder canyons (Figure 5B) suggests a contourite-dominated mixed system. These features indicate sustained bottom current activity (Hernández-Molina et al., 2008; Rebesco et al., 2014). Submarine canyons associated with the headscarp at the downdip part of the plastered drift suggest that slope failure is likely due to oversteepening as the drift accumulates (e.g., Brackenridge et al., 2020). Therefore, this segment is classified as a contourite-dominated mixed system as bottom currents control depositional morphology (Figure 9).



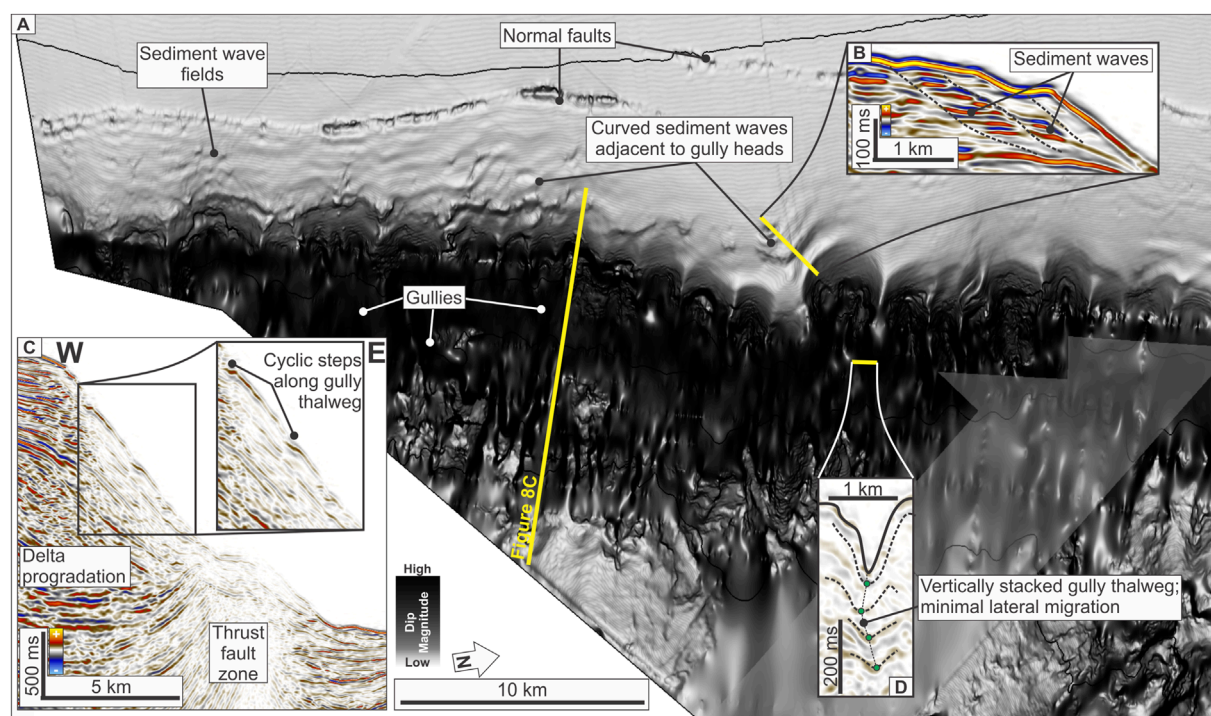


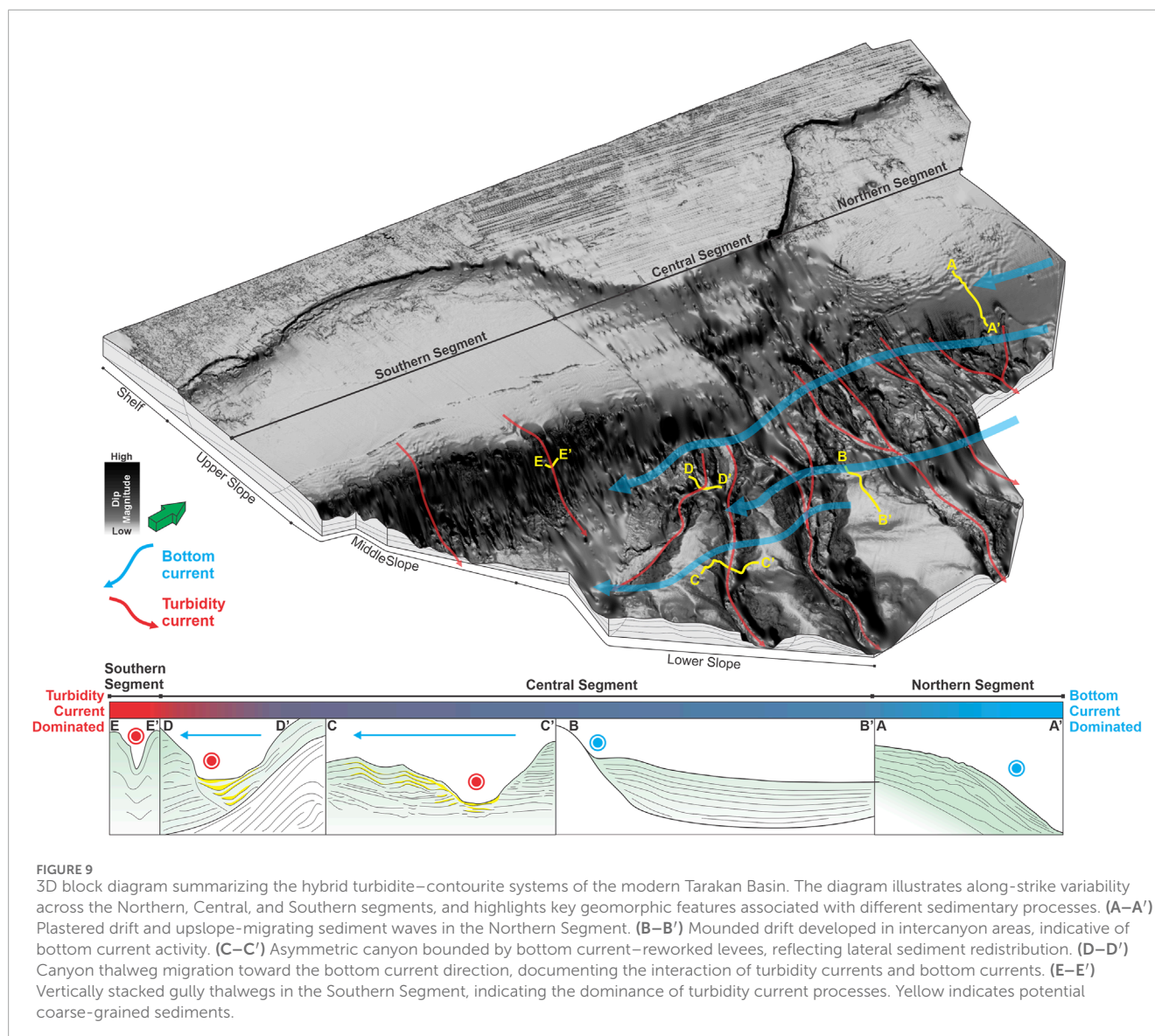
**FIGURE 8**  
**(A)** Dip magnitude map of the Southern Segment, highlighting gully networks and associated sediment wave fields. **(B)** Seismic profile across upslope-migrating sediment waves. **(C)** Seismic section along a gully thalweg, showing internal cyclic steps interpreted as the product of turbidity flows. **(D)** Vertically stacked gully thalwegs with no lateral offset, suggesting minimal influence from bottom currents. Green dots represent gully thalwegs.

The Central Segment presents a more complex expression of process interactions (Figure 9). The radial arrangement of the HILA submarine canyons and the presence of inter-canyon contouritic drifts and sediment waves represent a synchronous interaction regime (Fuhrmann et al., 2022; Kiswaka et al., 2025; Lu et al., 2021a; Palamenghi et al., 2015; Rodrigues et al., 2022b; Schattner et al., 2024). Here, sediment gravity flows delivered by slope failures and canyon-forming processes interact coevally with alongslope bottom currents. The canyon–drift morphology, with high-amplitude reflectors (HARs) extending from the thalweg into the drift bodies (Figure 6), is similar with the characteristics of synchronous systems described by Rodrigues et al. (2022b), where the deviation and redistribution of turbidity plumes by bottom currents result in lateral facies variation and mounded drift growth (Lu et al., 2021a; Miramontes et al., 2020). Updip, the lateral offset of thalwegs (Figures 7A–C) near canyon heads and the occurrence of cyclic steps (Figure 6C) reflect active flow interactions. Meanwhile, downdip, high-energy turbidity currents are deflected by alongslope currents, forcing sediment redistribution toward the drift flanks forming the bottom current-reworked levee (Figure 7D; Fuhrmann et al., 2022; Kiswaka et al., 2025; Miramontes et al., 2020; Rodrigues et al., 2022a; Sansom, 2018). The coincidence between moat locations and the underlying thrusts suggests structural influence on the mounded drifts growth (Figure 7E; Hernández-Molina et al., 2008; Rebesco et al., 2014). The presence of these moats and mounded drifts at depths >1,500 m may serve as indirect evidence of deep isolated current circulation

within the Sulawesi Sea, which remains poorly constrained and need further investigation (Gordon et al., 2003; O'Driscoll and Kamenkovich, 2009).

The Southern Segment is more reflective of a turbidite-dominated mixed system (Figure 9). The presence of linear gullies and associated cyclic steps along their thalwegs indicates sustained, low-density, mud-rich turbidity flows sourced from the active delta system upslope. Sediment waves near gully heads, some of which migrate upslope and curve parallel to the gullies, suggest minor modification by bottom currents. However, the overall morphology and lack of lateral thalweg migration support a system dominated by gravity-driven sediment transport, with limited alongslope influence. This geometry fits with the models proposed by Rodrigues et al. (2022b), where steep slope gradients and strong deltaic input favor turbidite dominance and inhibit significant drift development or system migration.

These three segments exemplify the continuum of mixed system types—from contourite-dominated to synchronous hybrid to turbidite-dominated—each shaped by different balances of sediment supply, tectonic confinement, and bottom current strength and variability (Figure 9). This segmentation is consistent with findings from other margins such as the South China Sea (Gong et al., 2015; Gong et al., 2016; Palamenghi et al., 2015), and East Africa (Fonnesu et al., 2020; Fuhrmann et al., 2022; Kiswaka et al., 2025; Lu et al., 2021a; Sansom, 2018).



## 5.2 Analogue for petroleum and carbon storage systems

This study provides insight into the present-day seafloor processes shaping the Tarakan Basin, based on seismic sedimentology analysis. While it does not directly characterize subsurface reservoirs, the observed hybrid features—such as sediment waves, mounded drifts, and submarine canyons—offer important analogues for interpreting older sedimentary systems. Given that both the Tarakan Delta and the ITF (and its associated deeper currents) have likely been active since at least the Miocene (Gallagher et al., 2024), the conditions for interacting downslope and upslope processes may have existed during the basin's geological history. This raises the possibility that ancient hybrid systems, formed under similar dynamic conditions, are preserved at depth.

Globally, hybrid turbidite–contourite systems are increasingly recognized as prospective targets for petroleum exploration and subsurface storage. In the Eocene–Oligocene interval of the Santos

Basin, sand-rich contouritic beds have demonstrated net-to-gross ratios of 15%–25%, locally reaching up to 35%, with good porosity and lateral continuity (Mutti et al., 2014; Viana et al., 2007). Similarly, the Coral and Mamba gas fields along the northern Mozambican margin represent successful hydrocarbon discoveries within mixed systems. These fields contain an estimated  $2.32 \times 10^{12} \text{ m}^3$  of recoverable gas, with an average porosity of 16.9% and net-to-gross ratio of 82% (Fonnesu et al., 2020). The reservoirs are associated with asymmetric, migrating fan lobes, formed through synchronous interactions between downslope turbidity currents and upslope bottom currents. Kiswaka et al. (2025) also emphasize that reservoir quality varies across different intervals of hybrid systems, with higher seismic amplitudes potentially indicating better reservoir potential. These analogues underscore the exploration potential of hybrid systems, particularly where fine-grained contourites interleave with or drape over sand-rich turbidite units.

In the Tarakan Basin, similar high-amplitude reflections in canyon and drift settings suggest facies variability that could be favorable for both hydrocarbon reservoirs and carbon capture and

storage (CCS). The combination of sand-prone geometries and continuous mud-prone drapes may offer effective reservoir–seal pairs, especially in settings where structural and geomorphic trapping mechanisms coincide (Figure 9). Although further stratigraphic, sedimentological, and petrophysical data are required to evaluate reservoir quality, storage capacity, and injectivity at depth, the present-day seafloor of the Tarakan Basin provides a valuable analogue. The combination of canyon-associated HARs, drift geometries, and segment-scale variability represent a first step toward identifying the potential subsurface storage targets shaped by hybrid sedimentary processes.

## 6 Conclusion

The deepwater Tarakan Basin offers a valuable natural laboratory for investigating hybrid turbidite–contourite systems in a tectonically active, delta-fed margin. This study presents an initial characterization of its seafloor morphology using 3D seismic data, revealing three distinct geomorphic segments. The Northern Segment is contourite-dominated, the Central Segment reflects synchronous interactions between gravity flows and bottom currents, and the Southern Segment is shaped primarily by turbidity currents. These spatial variations highlight how structural setting, sediment supply, and oceanographic forcing combine to generate diverse depositional architectures along a single continental slope.

The geomorphic variability observed in this study has important implications for subsurface resource development. Canyon fills and inter-canyon drifts with high-amplitude seismic reflections may represent potential hydrocarbon reservoirs or carbon storage sites, especially where sand-prone and mud-prone facies are vertically and laterally juxtaposed. Understanding the spatial distribution of these features enhances predictive models of reservoir and seal prospectivity.

This study provides foundational insights into modern hybrid sedimentary systems in the Tarakan Basin. However, further research is needed to better quantify the interactions between turbidity flows and bottom currents. Future work should include sedimentary facies analysis from well logs and core data to validate seismic interpretations and refine depositional models. Integration with paleoceanographic reconstructions will further improve understanding of the hybrid systems evolution.

## Data availability statement

The data that support the findings of this study were provided by Information and Data Centre, Ministry of Energy and Mineral Resources (PUSDATIN ESDM) of the Republic of Indonesia and are publicly available for request through [datamigas.esdm.go.id](http://datamigas.esdm.go.id).

## References

Advokaat, E. L., Marshall, N. T., Li, S., Spakman, W., Krijgsman, W., and Van Hinsbergen, D. J. (2018). Cenozoic rotation history of Borneo and Sundaland, SE Asia

## Author contributions

HN: Methodology, Conceptualization, Writing – review and editing, Software, Visualization, Formal Analysis, Writing – original draft. HM: Conceptualization, Supervision, Writing – review and editing, Visualization, Data Curation.

## Funding

The author(s) declare that financial support was received for the research and/or publication of this article. The University of Bergen (UiB) provided funding for the article processing charge through its Publication Fund for Open Access.

## Acknowledgments

We thank the Information and Data Centre, Ministry of Energy and Mineral Resources (PUSDATIN ESDM) of the Republic of Indonesia for providing the 3D seismic reflection through the Migas Data Repository (MDR), and Schlumberger for granting software license to University of Bergen and Universitas Pertamina. Our appreciation extends to colleagues at LEMIGAS and Pertamina Hulu Energi (PHE) for their broader and in-depth research on the Tarakan Basin, which provided valuable context and insight. We thank the editor for handling this article and the three reviewers for their constructive feedback, which significantly improved the manuscript.

## Conflict of interest

The authors declare that the research was conducted in the absence of any commercial or financial relationships that could be construed as a potential conflict of interest.

## Generative AI statement

The author(s) declare that no Generative AI was used in the creation of this manuscript.

## Publisher's note

All claims expressed in this article are solely those of the authors and do not necessarily represent those of their affiliated organizations, or those of the publisher, the editors and the reviewers. Any product that may be evaluated in this article, or claim that may be made by its manufacturer, is not guaranteed or endorsed by the publisher.

revealed by paleomagnetism, seismic tomography, and kinematic reconstruction. *Tectonics* 37, 2486–2512. doi:10.1029/2018tc005010



- Alves, D. P., Maselli, V., Iacopini, D., Viana, A. R., and Jovane, L. (2023). Oceanographic exchanges between the southern and northern atlantic during the cenozoic inferred from mixed contourite-turbidite systems in the Brazilian equatorial margin. *Mar. Geol.* 456, 106975. doi:10.1016/j.margeo.2022.106975
- Amjadian, P., Neill, S. P., and Marti Barclay, V. (2023). Characterizing seabed sediments at contrasting offshore renewable energy sites. *Front. Mar. Sci.* 10, 1156486. doi:10.3389/fmars.2023.1156486
- Bailey, L. P., Clare, M. A., Hunt, J. E., Kane, I. A., Miramontes, E., Fonnesu, M., et al. (2024). Highly variable deep-sea currents over tidal and seasonal timescales. *Nat. Geosci.* 17, 787–794. doi:10.1038/s41561-024-01494-2
- Brackenridge, R. E., Nicholson, U., Sapiie, B., Stow, D., and Tappin, D. R. (2020). “Indonesian throughflow as a preconditioning mechanism for submarine landslides in the Makassar Strait,” in *Subaqueous mass movements and their consequences: advances in process understanding, monitoring and hazard assessments*. (London: Geological Society of London).
- Brown, A. R. (2011). *Interpretation of three-dimensional seismic data*. Society of Exploration Geophysicists and American Association of Petroleum Geologists.
- Erdi, A., Jackson, C. A. L., and Soto, J. I. (2023). Extensional deformation of a shale-dominated delta: Tarakan Basin, offshore Indonesia. *Basin Res.* 35, 1071–1101. doi:10.1111/bre.12747
- Ericson, D., Ewing, M., and Heezen, B. C. (1952). Turbidity currents and sediments in north atlantic. *AAPG Bull.* 36, 489–511. doi:10.1306/3d934415-16b1-11d7-8645000102c1865d
- Fang, G., Wang, Y., Wei, Z., Fang, Y., Qiao, F., and Hu, X. (2009). Inter-ocean circulation and heat and freshwater budgets of the South China Sea based on a numerical model. *Dyn. Atmos. Oceans* 47, 55–72. doi:10.1016/j.dynatmoce.2008.09.003
- Fan, W., Jian, Z., Bassinot, F., and Chu, Z. (2013). Holocene centennial-scale changes of the Indonesian and South China sea throughflows: evidences from the Makassar Strait. *Glob. Planet. Change* 111, 111–117. doi:10.1016/j.gloplacha.2013.08.017
- Fan, W., Jian, Z., Chu, Z., Dang, H., Wang, Y., Bassinot, F., et al. (2018). Variability of the Indonesian throughflow in the Makassar strait over the last 30 ka. *Sci. Rep.* 8, 5678. doi:10.1038/s41598-018-24055-1
- Fonnesu, M., Palermo, D., Galbiati, M., Marchesini, M., Bonamini, E., and Bendias, D. (2020). A new world-class deep-water play-type, deposited by the syndepositional interaction of turbidity flows and bottom currents: the giant Eocene Coral Field in northern Mozambique. *Mar. Petroleum Geol.* 111, 179–201. doi:10.1016/j.margeo.2019.07.047
- Fuhrmann, A., Kane, I., Schomacker, E., Clare, M., and Pontén, A. (2022). Bottom current modification of turbidite lobe complexes. *Front. Earth Sci.* 9, 752066. doi:10.3389/feart.2021.752066
- Gallagher, S. J., Auer, G., Brierley, C. M., Fulthorpe, C. S., and Hall, R. (2024). Cenozoic history of the Indonesian gateway. *Annu. Rev. Earth Planet. Sci.* 52, 581–604. doi:10.1146/annurev-earth-040722-111322
- Gee, M., Uy, H., Warren, J., Morley, C., and Lambiasi, J. (2007). The Brunei slide: a giant submarine landslide on the North West Borneo Margin revealed by 3D seismic data. *Mar. Geol.* 246, 9–23. doi:10.1016/j.margeo.2007.07.009
- Gong, C., Wang, Y., Xu, S., Pickering, K. T., Peng, X., Li, W., et al. (2015). The Northeastern South China Sea margin created by the combined action of down-slope and along-slope processes: processes, products and implications for exploration and paleoceanography. *Mar. Petroleum Geol.* 64, 233–249. doi:10.1016/j.margeo.2015.01.016
- Gong, C., Wang, Y., Zheng, R., Hernández-Molina, F. J., Li, Y., Stow, D., et al. (2016). Middle Miocene reworked turbidites in the Baiyun Sag of the pearl river mouth basin, northern south China sea margin: processes, genesis, and implications. *J. Asian Earth Sci.* 128, 116–129. doi:10.1016/j.jseas.2016.06.025
- Gordon, A. L. (2005). Oceanography of the Indonesian seas and their throughflow. *Oceanography* 18, 14–27. doi:10.5670/oceanog.2005.01
- Gordon, A. L., Giulivi, C. F., and Ilahude, A. G. (2003). Deep topographic barriers within the Indonesian seas. *Deep Sea Res. Part II Top. Stud. Oceanogr.* 50, 2205–2228. doi:10.1016/S0967-0645(03)00053-5
- Hall, R., and Nichols, G. (2002). “Cenozoic sedimentation and tectonics in Borneo: climatic influences on orogenesis,” in *Sediment flux to basins: causes, controls and consequences*. Editors S. J. Jones, and L. E. Frostick (London: Geological Society).
- Harishidayat, D., Niyazi, Y., Stewart, H. A., Al-Shuhail, A., and Jamieson, A. J. (2024). Submarine canyon development controlled by slope failure and oceanographic process interactions. *Sci. Rep.* 14, 18486. doi:10.1038/s41598-024-69536-8
- Hermansyah, H., Atmadipoera, A., Prartono, T., Jaya, I., and Syamsudin, F. (2019). Energetics of internal tides over the Sangihe-Talaud ridge-Sulawesi sea. *J. Phys. Conf. Ser.* 1341, 082001. doi:10.1088/1742-6596/1341/8/082001
- Hernández-Molina, F., Llave, E., and Stow, D. (2008). Continental slope contourites. *Dev. Sedimentol.* 60, 379–408. doi:10.1016/S0070-4571(08)10019-X
- Hidayati, S., Guritno, E., Argenton, A., Ziza, W., and Del Campana, I. (2007). *Revised structural framework of the tarakan sub-basin, northeast kalimantan-Indonesia. Thirty-first annual Convention and exhibition, Indonesian petroleum association*. Jakarta: AAPG Datapages.
- Hollister, C. D., and Heezen, B. C. (1972). “Geologic effects of ocean bottom currents: western North Atlantic,” in *Studies in physical oceanography*. Editor A. L. Gordon (New York, NY: Gordon and Breach Science Publishers).
- Jobe, Z. R., Lowe, D. R., and Uchytel, S. J. (2011). Two fundamentally different types of submarine canyons along the continental margin of Equatorial Guinea. *Mar. Petroleum Geol.* 28, 843–860. doi:10.1016/j.margeo.2010.07.012
- Kiswaka, E. B., Harishidayat, D., Mkinga, O. J., and Gama, J. W. (2025). Hybrid turbidite-contourite system on the upper-slope continental margin of the offshore southern Tanzania. *J. Afr. Earth Sci.* 222, 105496. doi:10.1016/j.jafrearsci.2024.105496
- Krisnabudhi, A., Sapiie, B., Riyanto, A. M., Gunawan, A., and Rizky, F. F. (2022). Compression therapy, autonomic nervous system, and heart rate variability: a narrative review and our preliminary personal experience. *Phlebol. Mesozoic-Cenozoic Stratigr. Tect. Dev. South. Gt. Tarakan Basin Northeast Borneo Indonesia* 37, 739–753. doi:10.1177/02683555221135321
- Lentini, M. R., and Darman, H. (1996). *Aspects of the Neogene tectonic history and hydrocarbon geology of the Tarakan Basin. 25th annual convention, Indonesian petroleum association*. Jakarta: AAPG Datapages.
- Liu, S., Liang, Z., Zhang, B., Su, H., Lei, Z., and Su, M. (2022). Carbonate contourite drifts in the southwest South China Sea: sedimentary, paleoceanographic and economic implications. *Front. Mar. Sci.* 9, 946231. doi:10.3389/fmars.2022.946231
- Loneragan, L., Jamin, N. H., Jackson, C. A.-L., and Johnson, H. D. (2013). U-shaped slope gully systems and sediment waves on the passive margin of Gabon (West Africa). *Mar. Geol.* 337, 80–97. doi:10.1016/j.margeo.2013.02.001
- Lunt, P., and Madon, M. (2017). Onshore to offshore correlation of northern Borneo; a regional perspective. *Bull. Geol. Soc. Malays.* 64, 101–122. doi:10.7186/bgs64201710
- Lu, Y., Luan, X., Shi, B., Ran, W., Lü, F., Wang, X., et al. (2021a). Migrated hybrid turbidite-contourite channel-lobe complex of the late Eocene rovuma basin, East Africa. *Acta Oceanol. Sin.* 40, 81–94. doi:10.1007/s13131-021-1750-1
- Lu, Y., Shi, B., Maselli, V., Luan, X., Xu, X., Shao, D., et al. (2021b). Different types of gravity-driven flow deposits and associated bedforms in the Upper Bengal Fan, offshore Myanmar. *Mar. Geol.* 441, 106609. doi:10.1016/j.margeo.2021.106609
- Maulin, H. B., Sapiie, B., and Gunawan, I. (2019). “The Neogene deformation, unconformity surfaces and uplift features in delta tectonics, Tarakan Sub-Basin,” in *Forty-third annual convention and exhibition, Indonesian petroleum association*. Jakarta.
- Mcgilvery, T. M., and Cook, D. L. (2013). “The influence of local gradients on accommodation space and linked depositional elements across a stepped slope profile, offshore Brunei,” in *Shelf margin deltas and linked down slope petroleum systems—global significance and future exploration potential*. Editors H. H. Roberts, N. C. Rosen, R. H. Fillon, and J. B. Anderson (Tulsa, OK: SEPM Society for Sedimentary Geology). doi:10.5724/gcs.03.23.0387
- Miramontes, E., Eggenhuisen, J. T., Jacinto, R. S., Poneti, G., Pohl, F., Normandeau, A., et al. (2020). Channel-levee evolution in combined contour current–turbidity current flows from flume-tank experiments. *Geology* 48, 353–357. doi:10.1130/g47111.1
- Morley, R. J., Morley, H. P., and Swiecicki, T. (2017). *Constructing Neogene palaeogeographical maps for the Sunda region. South east asia petroleum exploration society (SEAPEX) conference*. Singapore: American Association of Petroleum Geologists.
- Mourlot, Y., Calvès, G., Clift, P. D., Baby, G., Chaboureaud, A.-C., and Raison, F. (2018). Seismic stratigraphy of cretaceous eastern central Atlantic ocean: basin evolution and paleoceanographic implications. *Earth Planet. Sci. Lett.* 499, 107–121. doi:10.1016/j.epsl.2018.07.023
- Mutti, E., Cunha, R. S., Bulhões, E., Arienti, L. M., and Viana, A. R. (2014). *Contourites and turbidites of the Brazilian marginal basins, 51069*. Tulsa, OK: American Association of Petroleum Geologists (AAPG), 1–46.
- Nugraha, H. D., Jackson, C. A.-L., Johnson, H. D., and Hodgson, D. M. (2020). Lateral variability in strain along the toewall of a mass transport deposit: a case study from the Makassar Strait, offshore Indonesia. *J. Geol. Soc.* 177, 1261–1279. doi:10.1144/jgs2020-071
- Nugraha, H. D., Jackson, C. A. L., Johnson, H. D., Hodgson, D. M., and Reeve, M. T. (2019). Tectonic and oceanographic process interactions archived in Late Cretaceous to present deep-marine stratigraphy on the Exmouth Plateau, offshore NW Australia. *Basin Res.* 31, 405–430. doi:10.1111/bre.12328
- O'Driscoll, K. T., and Kamenkovich, V. M. (2009). Dynamics of the Indonesian seas circulation. Part I—The influence of bottom topography on temperature and salinity distributions. *J. Mar. Res.* 67, 119–157. doi:10.1357/002224009789051236
- Palamenghi, L., Keil, H., and Spiess, V. (2015). Sequence stratigraphic framework of a mixed turbidite-contourite depositional system along the NW slope of the South China Sea. *Geo-Marine Lett.* 35, 1–21. doi:10.1007/s00367-014-0385-z
- Rebesco, M., Hernández-Molina, F. J., Van Rooij, D., and Wählin, A. (2014). Contourites and associated sediments controlled by deep-water circulation processes: state-of-the-art and future considerations. *Mar. Geol.* 352, 111–154. doi:10.1016/j.margeo.2014.03.011
- Rodrigues, S., Deptuck, M., Kendall, K., Campbell, C., and Hernández-Molina, F. (2022a). Cretaceous to Eocene mixed turbidite-contourite systems offshore Nova Scotia (Canada): spatial and temporal variability of down-and along-slope processes. *Mar. Petroleum Geol.* 138, 105572. doi:10.1016/j.margeo.2022.105572



- Rodrigues, S., Hernández-Molina, F., Fonnesu, M., Miramontes, E., Rebesco, M., and Campbell, D. (2022b). A new classification system for mixed (turbidite-contourite) depositional systems: examples, conceptual models and diagnostic criteria for modern and ancient records. *Earth-Sci. Rev.* 230, 104030. doi:10.1016/j.earscirev.2022.104030
- Sansom, P. (2018). Hybrid turbidite–contourite systems of the Tanzanian margin. *Pet. Geosci.* 24, 258–276. doi:10.1144/petgeo2018-044
- Sapiie, B., Furqan, T. A., Septama, E., Wardaya, P. D., and Gunawan, I. (2021). *Mechanism of gravity-driven deformation using sandbox modeling: a case study of the tarakan sub-basin, east kalimantan*. Jakarta: Forty-Fifth Annual Convention and Exhibition, Indonesian Petroleum Association.
- Satyana, A. H. (2015). *Rifting history of the Makassar Straits: new constraints from wells penetrating the Basement and oils discovered in Eocene section-implications for further exploration of West Sulawesi Offshore*. Jakarta: Thirty-Ninth Annual Convention and Exhibition, Indonesian Petroleum Association.
- Schattner, U., Rocha, C. B., Ramos, R. B., Shtober-Zisu, N., Lobo, F. J., and De Mahiques, M. (2024). Lateral shift from turbidite-to contourite-dominated continental slope, a case study from southeast Brazil slope. *Geomorphology* 447, 109009. doi:10.1016/j.geomorph.2023.109009
- Susanto, R. D., and Gordon, A. L. (2005). Velocity and transport of the Makassar strait throughflow. *J. Geophys. Res. Oceans* 110. doi:10.1029/2004jc002425
- Trinh, N. B., Herrmann, M., Ulses, C., Marsaleix, P., Duhaut, T., To Duy, T., et al. (2024). New insights into the South China Sea throughflow and water budget seasonal cycle: evaluation and analysis of a high-resolution configuration of the ocean model SYMPHONIE version 2.4. *Geosci. Model Dev.* 17, 1831–1867. doi:10.5194/gmd-17-1831-2024
- Viana, A., Almeida, W., Nunes, M., and Bulhões, E. (2007). “The economic importance of contourites,” in *Economic and palaeoceanographic significance of contourite deposits*. Editors A. R. Viana, and M. Rebesco (London: Geological Society of London).
- Warchol, M. J., Pontén, A., and Furre, A. K. (2025). Stratigraphic controls on  $\delta_2$  migration at sleipner: an example from a basin-floor fan of the utsira formation. *Basin Res.* 37, e70018. doi:10.1111/bre.70018
- Wei, J., Li, M., Malanotte-Rizzoli, P., Gordon, A., and Wang, D. (2016). Opposite variability of Indonesian throughflow and South China Sea throughflow in the Sulawesi Sea. *J. Phys. Oceanogr.* 46, 3165–3180. doi:10.1175/jpo-d-16-0132.1
- Wu, N., Nugraha, H. D., Steventon, M. J., and Zhong, G. (2022). How do tectonics influence the initiation and evolution of submarine canyons? A case study from the Otway Basin, SE Australia. *J. Geol. Soc.* 179, jgs2021–jgs2170. doi:10.1144/jgs2021-170
- Wu, N., Zhong, G., Niyazi, Y., Wang, B., Nugraha, H. D., and Steventon, M. J. (2024). Transformation of dense shelf water cascade into turbidity currents: insights from high-resolution geophysical datasets. *Earth Planet. Sci. Lett.* 626, 118547. doi:10.1016/j.epsl.2023.118547
- Xu, D., and Malanotte-Rizzoli, P. (2013). The seasonal variation of the upper layers of the South China Sea (SCS) circulation and the Indonesian through flow (ITF): an ocean model study. *Dyn. Atmos. Oceans* 63, 103–130. doi:10.1016/j.dynatmoce.2013.05.002